Ocean Science Journal, Vol. 43 No. 1, 17-24(2008)

Article

Ocean Science Journal

http://osj.kr

Gas Exchange Rates Measured Using a Dual-Tracer (SF_6 and ^3He) Method in the Coastal Waters of Korea

Hyun-Woo Lee[1], Kitack Lee[1]*, and Duk-In Kaown[2]

[1]*School of Environmental Science and Engineering, Pohang University of Science and Technology, Pohang 790-784, Korea*
[2]*School of Earth and Environmental Sciences, Seoul National University, Seoul 151-747, Korea*

Received 3 September 2007; Revised 13 November 2007; Accepted 4 February 2008

Abstract – Over a period of 5 days between August 12 and 17, 2005, we performed a gas exchange experiment using the dual tracer method in a tidal coastal ocean located off the southern coast of Korea. The gas exchange rate was determined from temporal changes in the ratio of ^3He to SF_6 measured daily in the surface mixed layer. The measured gas exchange rate (k_{CO_2}), normalized to a Schmidt number of 600 for CO_2 in fresh water at 20°C, was approximately 5.0 cm h^{-1} at a mean wind speed of 3.9 m s^{-1} during the study period. This value is significantly less than those obtained from floating chamber-based experiments performed previously in estuarine environments, but is similar in magnitude to values obtained using the dual tracer method in river and tidal coastal waters and values predicted on the basis of the relationship between the gas exchange rate and wind speed (Wanninkhof 1992), which is generally applicable to the open ocean. Our result is also consistent with the relationship of Raymond and Cole (2001), which was derived from experiments carried out in estuarine environments using ^{222}Rn and chlorofluorocarbons along with measurements undertaken in the Hudson River, Canada, using SF_6 and ^3He. Our results indicate that tidal action in a microtidal region did not discernibly enhance the measured k_{CO_2} value.

Key words – gas exchange rate, SF_6, ^3He, dual tracer, coastal ocean

1. Introduction

Coastal seas play an important role in the global carbon cycle by linking the terrestrial and open-ocean carbon reservoirs, even though they account for just 7% of the surface area of the global ocean. Organic matter is generally produced in these coastal seas at rates significantly higher than those observed in the open oceans, reflecting high inputs and rapid turnover of nutrients from adjoining rivers (*e.g.* Mackenzie *et al.* 1998; Tsunogai *et al.* 1999; Chen *et al.* 2003, 2006; Thomas *et al.* 2004). The organic matter undergoes *in situ* biogeochemical transformation, sinks to the seafloor sediments within the coastal area, or is transported to the open ocean. In particular, an accurate knowledge of gas exchange rate is a key factor in determining the ability of coastal seas to absorb ever-increasing amounts of anthropogenic CO_2 in estuaries or coastal waters. However, there are few direct measurements of gas exchange rate in estuaries and coastal waters (Raymond and Cole 2001).

Measurements of the gas exchange rate in estuaries and tidal coastal waters have usually employed a floating chamber method (*e.g.* Borges *et al.* 2004), because such a method is simple to use and is considered likely to capture short-term variations in the gas exchange rate over an area of less than several square meters; however, a possible caveat associated with this method is that the deployment of the floating chamber on the surface of the river or estuary is likely to affect the turbulence and thereby biases measurements of the gas exchange rate (Matthew *et al.* 2003). Chlorofluorocarbons and ^{222}Rn have also been used, but accurate estimation of the mass balance of a tracer is far from simple because the processes that remove or add the tracer to the body of water are commonly too complex to fully comprehend (Roether and Kromer 1984).

The $SF_6/^3He$ deliberate dual tracer method can overcome many of the limitations described in the preceding paragraph. In the present study, we tagged a water mass with sulfur hexafluoride (SF_6) and helium-3 (^3He) within the surface

*Corresponding author. E-mail: ktl@postech.ac.kr

mixed layer of a tidal coastal ocean located off the southern coast of Korea and followed its subsequent pathway for 5 days to determine gas exchange rates. These results can be valuable because only a few SF_6/^{3}He dual tracer experiments have been conducted in rivers and tidal coastal oceans (*e.g.* Wanninkhof *et al.* 1993, 1997; Clark *et al.* 1994; Nightingale *et al.* 2000a). This lack of data severely limits our ability to verify previously published accounts of the relationship between the exchange rate and wind speed (*e.g.* Ramond and Cole 2001; Borges *et al.* 2004) derived from either the floating dome or non-dome methods for tidal estuarine and coastal environments.

In this paper, we report gas exchange rates derived from the temporal evolution of changes in the ratio of ^{3}He to SF_6 within the surface mixed layer of a tidal coastal ocean located off the southern coast of Korea. In addition, by comparing a limited number of SF_6/^{3}He-derived gas exchange rates with existing parameterizations derived from either the floating dome or non-dome methods, we are able to assess the accuracy of these latter methods as well as the degree to which surface turbulence associated with tidal activity enhances the rate of gas exchange.

2. Materials and Method

Calculation of the gas-exchange rate using dual tracer data

The absolute gas-exchange rate for either of ^{3}He and SF_6 can be calculated from changes in the ratio of ^{3}He to SF_6 over time within the wind-driven mixed layer and the ratio of the Schmidt numbers (*Sc*) for the two gases (Sc_{SF_6}, $Sc_{^3He}$), as described by the following equation (Watson *et al.* 1991; Wanninkhof *et al*. 1993):

$$k_{^3He} = H/\Delta t \ln(R_{t_1}/R_{t_2})/[1-(Sc_{^3He}/Sc_{SF_6})^{-0.5}] \quad (1)$$

where $k_{^3He}$ is the transfer rate of ^{3}He across the air-sea interface; *H* is the mean mixed-layer depth in meters over the time interval (Δt) between t_1 and t_2; R_{t_1} and R_{t_2} are the ratios of ^{3}He and SF_6 concentrations in the surface mixed layer at t_1 and t_2, as corrected for natural background concentrations that represent the attainable values when seawater is in equilibrium with the atmosphere prior to the release of the tracer gases; and -0.5 is the *Sc* exponent (Ledwell 1984; Jähne *et al.* 1987; Watson *et al*. 1991).

Tracer (SF_6 and ^{3}He) injection

The study site chosen for the present experiment is located near the island of Naro-do off the southern coast of Korea (Fig. 1). A mixture of approximately 20 mol of SF_6 (99.7% v/v) and 0.06 mol of ^{3}He (0.3% v/v) was released at a depth of 1.5 m over a 2 km × 1 km area by bubbling the mixture of two gases into the water column through 250 μm-perforated hose (3 m long and 0.5 mm i.d.) that was wrapped around a perforated plastic cylinder (0.5 m long and 20 cm i.d.). The gas injection was performed using an even track spacing with ~100 m between tracks immediately aft of an auxiliary ship's propeller as the ship moved over a 2 km^2 rectangular grid. The auxiliary vessel was used to avoid cross contamination of the sampling and measurement apparatus aboard the main ship with the concentrated tracer gases. During gas injection, a global positioning system (GPS) buoy was deployed at the center of the SF_6 patch to follow the movement of the patch during the tracer experiment.

Tracer analysis

An automated sampling and analysis system for SF_6 in surface waters (*e.g.* Wanninkhof *et al*. 2004; Koo *et al*. 2005) was used as the primary method of mapping the advection and dispersion of the tracer patch and thereby locating the center of the patch on a daily basis. The center of the patch generally corresponded to the site of the daily maximum concentration of SF_6.

To determine daily trends in the ratio of ^{3}He to SF_6, seawater samples were collected daily from three hydrocasts near the center of the patch. The three casts were made at approximately even time intervals from morning to evening. SF_6 analysis was undertaken immediately onboard the vessel, whereas ^{3}He analysis was carried out on shore at a later date. The onboard SF_6 analysis for batch samples was performed following the measurement procedure described by Kim *et al*. (2005). The reproducibility of discrete SF_6 measurements was better than 10%, which was mostly derived from the errors of syringe sample volume, and the relatively inconsistent injected gas volume.

The shore-based ^{3}He analysis was performed following the procedure described by Lott and Jenkins (1984) at the Seoul National University noble gas analysis facility 10 months following the completion of the cruise. The precision of ^{3}He measurements was approximately ±0.8%, as determined on the basis of analysis of air standards.

Measurements of the He isotope ratio were accurate to within ±0.25% and were corrected for instrumental linearity that was determined against measurements of air standards. The fact that the ^{4}He contents of the analyzed seawater samples were approximately constant (within ±4%) for all analyzed samples indicates that air contamination during the sampling and extraction was likely to have been insignificant.

Wind speed

Wind speeds (U_Z, m s^{-1}) were measured onboard using a sonic anemometer that was mounted approximately 18 m above the sea level on the *R/V* Ieodo's forward bow mast. Under the assumption of a neutrally stable boundary layer and a logarithmic wind profile, wind data were corrected to a height of 10 m (U_{10}) above the sea level using $U_{10} = U_Z [1+(C_{d10})^{0.5} / k \ln (10/z)]$ (Donelan 1990), where C_{d10} is a drag coefficient of 1.2×10^{-3} at 10 m height (Large and Pong, 1981), k is the Von Karman constant of 0.4, and z is the height above the sea level (m).

3. Results and Discussion

Environmental conditions at the study site

The waters between the islands of Naro-do and Kumo-do were chosen as a study site for the present gas exchange experiment (Fig. 1). The study site is open to offshore waters to the south but has limited access to the inner bay to the north because of the presence of several islands between the inner bay and the study site. During the study period (August 2004), the physical characteristics of waters within the study site were mainly controlled by the interaction of inshore waters with offshore waters whose properties are similar to those of the Tsushima warm current (Park *et al.* 2005). The front that formed between these two contrasting water masses alternatively moved toward inshore and offshore on a daily basis, driven largely by daily tidal activity.

We released the dual tracers into the inshore waters to avoid inadvertent loss of the tracer patch to open ocean via the Tsushima warm current that usually flows in a northeasterly direction.

Over the study period, the hourly mean wind speeds (U_{10}) within the study site ranged from 0.4 to 7.5 m s^{-1}, with a mean value of 3.9 m s^{-1} (Fig. 2a). The wind blew mainly from the south over the entire study period, except for the fifth day of the study period when the prevailing direction

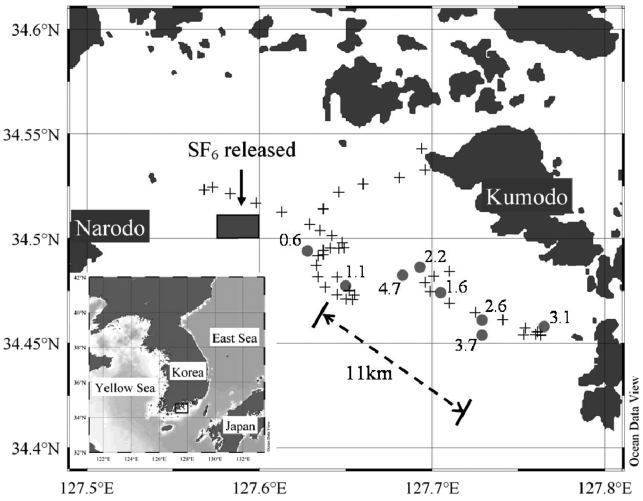

Fig. 1. Map of the study site showing the locations of the daily maximum SF_6 concentrations in the surface mixed layer (grey circles; experimental days are given next to each circle) and the GPS buoy (cross symbols). The location at which the tracer was released is shown by a grey rectangle. The dashed line indicates the mean distance that a water parcel travels between the ebb and flood tides.

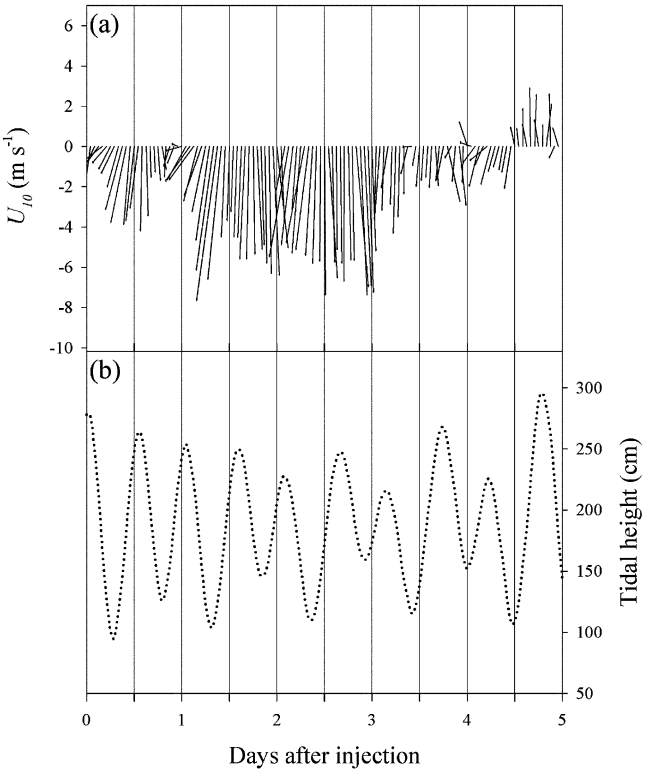

Fig. 2. Time Records of (a) wind velocities (m s^{-1}) and (b) tidal heights (cm) observed during the study experiment. Tidal heights were measured in Yeosu near the site.

of U_{10} suddenly switched from south to north. Overall, the lower mean U_{10} recorded during the study period indicated

that wind-induced turbulence was likely to have been minor at the study site. And the tracer patch experienced a spring-neap range of 1 to 3 m, with a mean water level difference of approximately 2 m (Fig. 2b). As we did not directly measure the tidal speed at the study site, we inferred it from the ADCP measurements conducted within waters located inshore of the study site in the summer of 2004 (Hahm *et al.* 2005). The estimated tidal speed ranged from 20 to 35 cm s^{-1} for spring tide and 5 to 15 cm s^{-1} for neap tide.

Evolution of the SF_6/^{3}He patch

Daily mapping of the spatial extent of the tracer patch indicated that the center of the patch alternatively moved in northwesterly and southeasterly directions during flood and ebb tides, respectively (gray circles in Fig. 1). This movement pattern of the patch center was confirmed independently from the evolution of GPS buoy positions (cross symbols in Fig. 1). The GPS buoy remained within the patch on Day 1 but deviated significantly from the patch during Days 2 and 3. We then recovered the buoy and repositioned it at the patch center; thereafter, the buoy remained within the patch.

The maximum SF_6 concentration within the mixed layer at the patch center decreased rapidly from ln [SF_6] = 10 (~20,000 fmol kg^{-1}) on Day 1 to ln [SF_6] = 5 (~140 fmol kg^{-1}) on Day 5 (Fig. 3a). The decrease in surface SF_6 concentrations over the 5-day study period was associated with three distinct processes: gas exchange with the atmosphere ($L_{AIR\text{-}SEA}$), lateral diffusion ($L_{DIFFUSION}$), and deepening of the mixed layer ($L_{DEEPING}$). The deepening of the mixed layer induces mixing with subsurface waters that contain no SF_6, leading to a reduction in SF_6 within the mixed layer; however, this effect is likely to be minimal because the mean mixed layer depth of approximately 4.5 m remained unchanged throughout the study period. Thus, the evolution of SF_6 concentration in the surface mixed layer was primarily determined by the combined loss of SF_6 due to air-sea gas exchange and horizontal diffusion. The reduction in SF_6 concentrations within the mixed layer associated with horizontal diffusion, $L_{DIFFUSION}$, was estimated from equivalent reductions measured at the patch center that were corrected for air-sea SF_6 loss estimated using the measured mean gas-exchange rate (k) described in the following section. The measured k yielded a loss of SF_6 to the atmosphere that accounted for less than 20% of the daily decrease in SF_6 concentrations during the study period, except for the last 2 days (Fig. 3b).

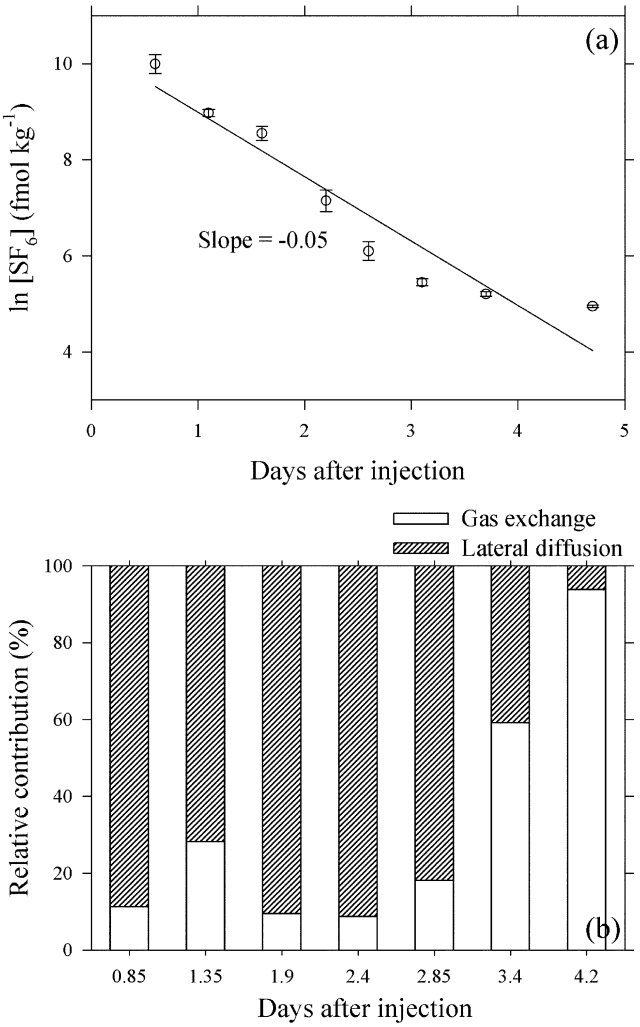

Fig. 3. (a) Underway measurements of the maximum surface SF_6 concentration ($[SF_6]_{max}$) at the patch center over the 5-day study period. The solid line is the best fit of the data and the error bars represent standard deviations from the mean of 7-10 SF_6 measurements. (b) Percentage loss of SF_6 at the patch center due to gas exchange (open bars) and lateral eddy diffusion (striped bars). Results were grouped into approximately 0.5-day intervals.

Determination of gas exchange rates

To accurately calculate k using Equation (1), the sets of ^{3}He and SF_6 data taken within the surface mixed layer must satisfy two conditions. First, both ^{3}He and SF_6 should be homogeneous in terms of their concentrations within the mixed layer and both should be free to transfer without restraint across the air-sea interface (Wanninkhof *et al.* 1993). In the present study, the mixed layer depth estimated on the basis of a vertical density gradient of $\Delta\sigma_\theta$ = 0.125 kg m^{-3} was approximately 4.5 m; at this depth, the SF_6 concentration was approximately 50% of the surface maximum (Fig. 4)

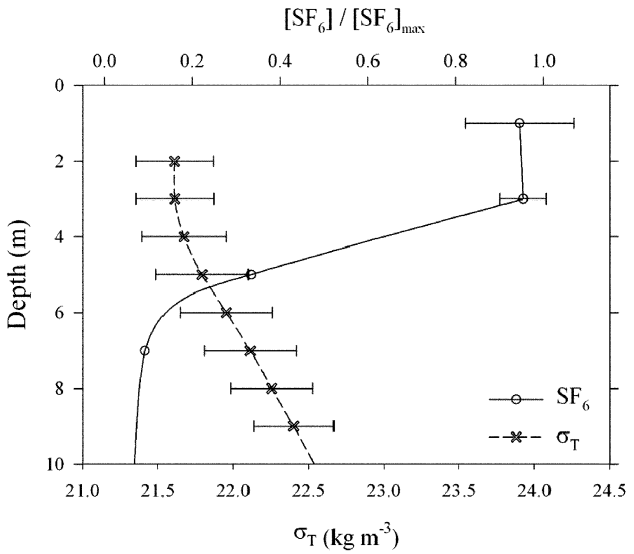

Fig. 4. Mean profiles of $[SF_6]/[SF_6]_{max}$ and sigma-t (σ_T). Five vertical SF_6 profiles were combined to generate the mean $[SF_6]/[SF_6]_{max}$ profile.

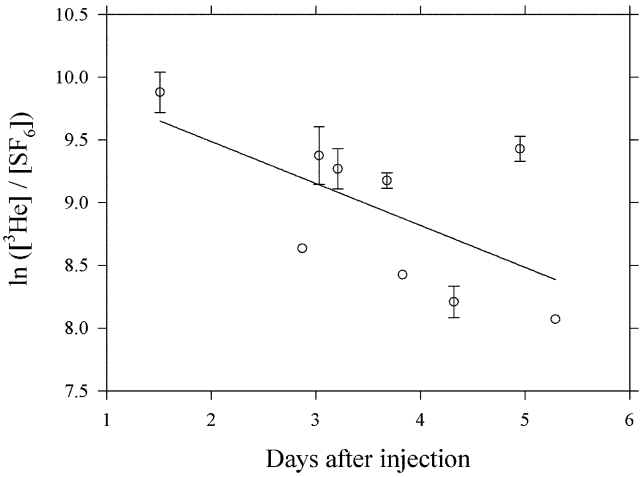

Fig. 5. Measured decrease in ln ($[^3He]/[SF_6]$) versus time (days) over the 5-day study period. Error bars represent the standard deviation from the mean for profiles down to 4.5 m that comprise either two to three samples or duplicate samples taken at the surface.

(see Nightingale *et al*. 2000b). Second, the formation of bubbles should be minimal to ensure an insignificant effect on *k*. The mean wind speed of 3.9 m s^{-1} observed over the study period was not strong enough to generate bubbles; accordingly, we used -0.5 of *Sc* exponent, which is commonly suitable for calculating *k* for surface conditions with some waves (Ledwell 1984).

The nine sets of ^3He and SF_6 measurements taken within the mixed layer satisfied the above two criteria; accordingly, we used these data sets to calculate *k*. The value of $k_{^3He}$ determined from the linear relationship between ln ($[^3He]/[SF_6]$) values and time, was 10.5 ± 5.1 cm h^{-1} (Fig. 5). To enable direct comparisons with previous dual tracer-based measurements of k_{CO_2}, the $k_{^3He}$ was then corrected to the Schmidt number of CO_2 in fresh water at 20 ºC using the following relationship:

$$k_{CO_2} = k_{^3He}(Sc_{CO_2}/Sc_{^3He})^{-0.5} \quad (2)$$

where the Schmidt number of CO_2 in fresh water at 20 ºC is 600. The resulting value of k_{CO_2} is 5.0 ± 2.4 cm h^{-1} at a mean U_{10} of 3.9 m s^{-1} over the 5-day study period. The uncertainty of ±2.4 cm h^{-1} in our k_{CO_2} value was due to scattering of the ratios of $[^3He]$ to $[SF_6]$ (Fig. 5). It is probable that some of the subsurface ^3He and SF_6 with different $[^3He]/[SF_6]$ ratios to those observed in the overlying surface waters diffused into the mixed layer and caused a non-systematic decrease in the ln ($[^3He]/[SF_6]$) ratio or that we sometimes sampled off the center where the ratio of $[^3He]$ to $[SF_6]$ might be smaller; however, we are unable to verify this possibility solely on the basis of presently available data.

Calculations of *k* using Equations (1) and (2) are sensitive to variations in the mixed layer depth because the magnitude of the calculated *k* is directly proportional to the mixed layer depth. Variations in measured mixed layer depth of approximately ±1 m over the present study period resulted in an uncertainty in the measured k_{CO_2} of approximately ±1.1 cm h^{-1}. Diel variations in the mixed layer depth associated with variations in the intensity of solar radiation also add a degree of uncertainty to the measured k_{CO_2}. The errors in the k_{CO_2} associated with diel variations in the mixed layer depth are comparable in magnitude to those caused by variations in the mixed layer depth over the 5-day study period. The measurement errors for SF_6 (±10%) and ^3He (±0.8%) lead to an error in the calculated k_{CO_2} of ±1.0 cm h^{-1}.

Comparison with previous estimates of gas exchange rate

We compared the k_{CO_2} value obtained in the present study with values obtained from previous dual tracer experiments performed in rivers and tidal coastal oceans (Fig. 6). Our k_{CO_2} value of 5.0 ± 2.4 cm h^{-1} at mean wind speed of 3.9 m s^{-1} is in good agreement with values measured upon the Hudson River, Canada (Clark *et al*. 1994), the Georges Bank, USA (Wanninkhof *et al.* 1993), and the west Florida

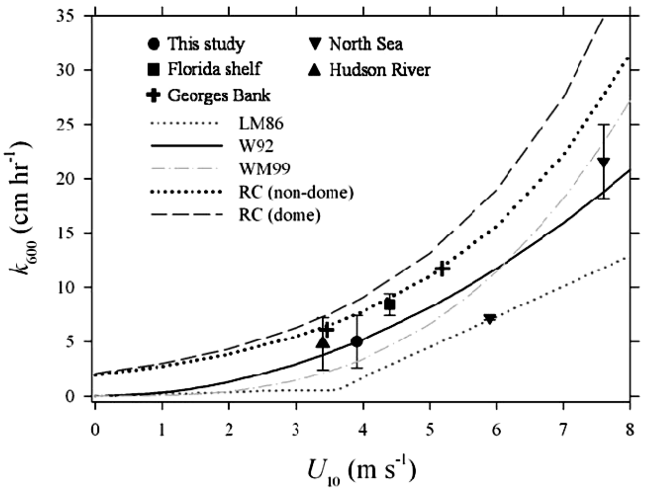

Fig. 6. Comparison of the short-term gas exchange parameterizations of Liss and Merlivat (1986, gray dotted line), Wanninkhof (1992, solid line), Wanninkhof and McGillis (1999, gray dashed-dotted line), Raymond and Cole (2001) using floating dome (dashed line) method with rates measured in a river (Hudson), and coastal waters (Florida shelf, Georges Bank, North Sea, and this study) using the ^{3}He/SF$_6$ method. Florida shelf data are from Wanninkhof *et al*. (1997), North Sea data are from Nightingale *et al.* (2000a), Georges Bank data are from Wanninkhof *et al*. (1993), and Hudson River data are from Clark *et al*. (1994).

shelf, USA (Wanninkhof *et al*. 1997), if all values are normalized to the common U_{10} using the k_{CO_2}-U_{10} parameterizations proposed by Wanninkhof (1992). Only two k_{CO_2} values measured upon the southern North Sea were used for comparison in Fig. 6, because other k_{CO_2} values reported by Nightingale *et al.* (2000a) were measured at values of U_{10} that were significantly greater than those at which other SF$_6$/^{3}He-based k_{CO_2} values were measured. The k_{CO_2} value at 7.7 m s^{-1} appears to be in reasonable agreement with five other dual tracer-based k_{CO_2} values when the k_{CO_2} values are normalized to the common U_{10} using the wind-speed-dependence of k_{CO_2} proposed by Wanninkhof (1992); however, the k_{CO_2} value at 5.9 m s^{-1} is significantly lower than the other dual tracer-based values. Although all five of the experiments considered above were performed in coastal environments of varying geographic settings, the measured k_{CO_2} values (except for one value measured upon the North Sea) largely follow a single trend as a function of wind speed ranging from 3 to 8 m s^{-1}.

We also compared the k_{CO_2} value obtained in the present study with predictions based on wind-gas exchange parameterizations that are commonly applicable to the open ocean (*e.g*. Liss and Merlivat 1986; Wanninkhof 1992; Wanninkhof and McGillis 1999). The present k_{CO_2} value is in reasonable agreement with the predicted values derived from the parameterization of Wanninkhof (1992) but is higher than the rate predicted by Liss and Merlivat (1986). This good overall agreement is somewhat fortuitous because these parameterizations were all forced to an intercept of $k_{CO_2} = 0$ at $U_{10} = 0$; thus, large differences in predicted k_{CO_2} values at high U_{10} become smaller with decreasing U_{10}.

All five of the SF$_6$/^{3}He-based k_{CO_2} values described above are in good agreement with the rates predicted from the parameterization, which was derived from ^{222}Rn- and CFC-based measurements in coastal environments and SF$_6$/^{3}He-based measurements undertaken upon the Hudson River (Ramond and Cole 2001); in contrast, the five values are significantly lower than the values obtained using the floating dome method (Fig. 6 or see Borges *et al*. 2004). Methodological differences are one possible explanation. For example, the deployment of a floating chamber might induce surface turbulence and thereby result in an overestimation of k_{CO_2}(Matthew *et al*. 2003; Upstill-Goddard 2006). Another possible factor is differences in the effect of tidal (or water) current on k_{CO_2}(Raymond and Cole 2001). In general, the effect of tidal current on the generation of surface turbulence, and thus k_{CO_2}, is proportional to the water depth to the power of -3/2 (O'Connor and Dobbins 1958). The present study was performed in water depths of ~30 m, whereas most of the floating chamber-based experiments were performed in water depths of less than 10 m. Therefore, assuming that the other factors were similar between the different studies, it is probable that tidal current had a less significant effect on the present tracer-based k_{CO_2} value than on previously determined floating chamber-based k_{CO_2} values.

Although the effects of tidal velocity and water depth can reasonably explain the discrepancies in k_{CO_2} values using the floating dome and SF$_6$/^{3}He methods, we cannot rule out the possibility that differences in fetch dependence, the breaking of micro-scale waves, and bubble ebullition also contribute to the observed discrepancies (Upstill-Goddard 2006).

In summary, the quantification of gas exchange rate at low wind speeds is important for biogeochemical mass balance studies that involve gaseous components in rivers, estuaries and coastal waters, where low wind speeds are common and air-sea CO_2 concentration gradients are large.

Therefore, our results are a valuable addition to existing data.

Acknowledgement

This work was financially supported by the National Research Laboratory Program (NRL) of the Korea Science and Engineering Foundation (KOSEF). Partial support was also provided by the AEBRC at POSTECH and the KOSEF (R01-2002-000-00549-0, 2004).

References

Borges, A.V., J.-P. Vanderborght, L.-S. Schiettecatte, F. Gazeau, S. F. Smith, B. Delille, and M. Frankignoulle. 2004. Variability of the gas transfer velocity of CO_2 in a macrotial estuary (the Scheldt). *Estuaries,* **27**, 593-603.

Chen, C.T.A., C.-T. Liu, W.S. Chuang, Y.J. Yang, F.-K. Shiah, T.Y. Tang, and S.W. Chung. 2003. Enhanced buoyancy and hence upwelling of subsurface Kuroshio waters after a typoon in the southern East China Sea. *Mar. Chem.*, **42**, 65-79.

Chen, C.T.A., W.-P. Hou, T. Gamo, and S.L. Wang. 2006. Carbonate-related parameters of subsurface waters in the West Philippine, South China and Sulu Seas. *Mar. Chem.*, **99**, 151-161.

Clark, J.F., R. Wanninkhof, P. Schlosser, and H.J. Simpson. 1994. Gas exchange rates in the tidal Hudson river using a dual tracer technique, *Tellus*, **46B**, 274-285.

Donelan, M.A. 1990. Air-Sea Interaction. p. 239292. In: *The Sea: Ocean Engineering Science 9*, ed. by B.LeMehaute and D. Hanes. John Wiley and Sons, Inc., NY.

Hahm, D., G. Kim, Y.-W. Lee, S.-Y. Nam, K.-R. Kim, and K. Kim. 2005. Tidal influence on the sea-to-air transfer CH_4 in the coastal ocean. *Tellus*, **58B**, 88-94.

Jähne, B., G. Heinz, and W. Dietrich. 1987. Measurements of the diffusion coefficients of sparingly soluble gases in water. *J. Geophys. Res*., **92**, 10767-10776.

Kim, D.-O., K. Lee, S.-D. Choi, H.-S. Kang, J.-Z. Zhang, and Y.-S. Chang. 2005. Determination of diapycnal diffusion rates in the upper thermocline in the North Atlantic Ocean using sulfur hexafluoride. *J. Geophys. Res.,* **110**, C10010. doi: 10.1029/2004JC002835.

Koo, C.-M., K. Lee, M. Kim, and D.-O. Kim. 2005. Automated system for fast and accurate analysis of SF_6 injected in the surface ocean. *Environ. Sci. Technol.*, **39**, 8427-8433.

Large, W.G. and S. Pong. 1981. Open ocean momentum flux measurements in moderate to strong winds. *J. Phys. Oceanogr.*, **11**, 324-336.

Ledwell, J.R. 1984. The variation of the gas transfer coefficient with molecular diffusivity. p. 293-302. In: *Gas Transfer at Water Surfaces*, ed. by W. Brutsaert and G. H. Jirka. Reidel, Norwell, Mass.

Liss, P.S. and L. Merlivat. 1986. Air-Sea gas exchange rates: Introduction and synthesis. p. 113-129. In: *The Role of Air-Sea Exchange in Geochemical cycling*, ed. by O. Buat-Ménatd. Reidel, Hingham, MA.

Lott, D.E. and W.J. Jenkins. 1984. An automated cryogenic charcoal trap system for helium isotope mass spectrometry. *Rev. Sci. Instrum.*, **55**, 1982-1988.

Mackenzie, F.T., A. Lerman, and L.M.B. Ver. 1998. Role of the continental margin in the global carbon balance during the past three centuries. *Geology*, **26**, 423-426.

Matthews, C.J.D., V.L.St. Louis, and R.H. Hesslein. 2003. Comparison of three techniques used to measure diffusive gas exchange from sheltered aquatic surfaces. *Environ. Sci. Technol.*, **37**, 772-780.

Nightingale, P.D., G. Malin, C.S. Law, A.J. Watson, P.S. Liss, M.I. Liddicoat, J. Boutin, and R.C. Upstill-Goddard. 2000a. In situ evaluation of air-sea gas exchange parameterization using novel conservative and volatile tracers. *Global Biogeochem. Cycles,* **14**, 373-387.

Nightingale, P.D., P.S. Liss, and P. Schlosser. 2000b. Measurements of air-sea gas transfer during an open ocean algal bloom. *Geophys. Res. Lett.*, **27**, 2117-2120.

O'connor, D. and W. Dobbins. 1958. Mechanism of reaeration in natural streams. *Trans. Amer. Soc. Civ. Eng*., **123**, 641-684.

Park, G.-H., K. Lee, C.-M. Koo, H.-W. Lee, C.-K. Lee, J.-S. Koo, T. Lee, S.-H. Ahn, H.-G. Kim, and B.-K. Park. 2005. A Sulfur hexafluoride-based Lagrangian study on initiation and accumulation of the red tide Cochlodinium polikrikoides in southern coastal waters of Korea. *Limnol. Oceanogr*., **50**, 578-586.

Raymond, P.A. and J.J. Cole. 2001. Gas exchange in rivers and estuaries: Choosing a gas transfer velocity. *Estuaries*, **24**, 312-317.

Roether, W. and B. Kromer. 1984. Optimal application of the radon deficit method to obtain air-sea gas exchange rates. In: *Gas Transfer at Water Surfaces*, ed. by W. Brutaert, G.H. Jirka, and D. Reidel. Norwell, Mass.

Thomas, H., Y. Bozec, K. Elkalay, and H.J.W. de Baar. 2004. Enhanced open ocean storage of CO_2 from shelf sea pumping. *Science*, ***304***, 1005-1008.

Tsunogai, S., S. Watanabe, and T. Sato. 1999. Is there a "continental shelf pump" for the absorption of atmospheric CO_2? *Tellus*, **51B**, 701-712.

Upstill-Goddard, R.C. 2006. Air-sea gas exchange in the coastal zone. *Estuar. Coas. Shelf Sci.*, **70**, 388-404.

Wanninkhof, R. 1992. Relationship between wind speed and gas exchange over the ocean. *J. Geophys. Res*., **97**, 7373-7382.

Wanninkhof, R., W. Asher, R. Weppernig, H. Chen, P. Schlosser, C. Langdon, and R. Sambrotto. 1993. Gas transfer experiment on

Georges Bank using two volatile deliberate traces. *J. Geophys. Res.*, **98**, 20237-20248.

Wanninkhof, R., G. Hitchcock, W.J. Wiseman, G. Vargo, P.B. Ortner, W. Asher, D.T. Ho, P. Schlosser, M.-L. Dickson, R. Masserini, K. Fanning, and J.-Z. Zhang. 1997. Gas exchange, dispersion, and biological productivity on the west Florida shelf: Results from a Lagrangian tracer study. *Geophys. Res. Lett.*, **24**, 1767-1770.

Wanninkhof, R. and W.R. McGillis. 1999. A cubic relationship between air-sea CO_2 exchange and wind speed. *Geophys. Res. Lett.*, **26**, 1889-1892.

Wanninkhof, R., K.F. Sullivan, and Z. Top. 2004. Air-sea gas transfer in the Southern Ocean. *J. Geophys. Res.,* **109**, C08S19. doi: 10.1029/2003JC001767.

Watson, A.J., R.C. Upstill-Goddard, and P.S. Liss. 1991. Air-sea exchange in rough and stormy seas measured by a dual tracer technique, *Nature*, **349**, 145-147.